· Review · Advances in Polar Science
doi: 10.13679/j.advps.2017.4.00256 December 2017 Vol. 28 No. 4: 256-267

# Progress in Antarctic marine geophysical research by the Chinese Polar Program

GAO Jinyao[1,2], SHEN Zhongyan[1,2], YANG Chunguo[1,2*], WANG Wei[1,2,3], JI Fei[1,2,4], WU Zhaocai[1,2], NIU Xiongwei[1,2], DING Weifeng[1,2], LI Dongxu[1,2] & ZHANG Qiao[1,2]

[1] Key Laboratory of Submarine Geosciences, State Oeanic Administration (SOA), Hangzhou 310012, China;
[2] Second Institute of Oceanography, SOA, Hangzhou 310012, China;
[3] Department of Earth Sciences, Zhejiang University, Hangzhou 310027, China;
[4] Chinese Antarctic Center of Surveying and Mapping, Wuhan University, Wuhan 430079, China

**Received 28 October 2017; accepted 30 December 2017**

**Abstract** Marine geophysical survey by the Chinese National Antarctic Research Expedition (CHINARE) began with the first science expedition in 1984/1985, although only four cruises were performed in the vicinity of the Antarctic Peninsula between then and 1991/1992. After a 20 year hiatus, Antarctic marine geophysical research was relaunched by the Chinese Polar Environmental Comprehensive Investigation and Assessment Programs (known simply as the Chinese Polar Program) in 2011/2012. Integrated geophysical surveys have been carried out annually since, in Prydz Bay and the Ross Sea. During the last 5 years, we have acquired about 5500 km of bathymetric, gravimetric, and magnetic lines; more than 1800 km of seismic reflection lines; and data from several heat flow and Ocean Bottom Seismometer (OBS) stations. This work has deepened understandings of geophysical features and their implications for geological tectonics and glacial history in Antarctica and its surrounding seas. Compiled Antarctic Bouguer and Airy isostatic gravity anomalies show different features of tectonics between the East Antarctic stability and West Antarctic activity. Calculated magnetic anomalies, heat flow anomalies and lithospheric anisotropy offshore of Prydz Bay may imply high heat capacity of mantle shielded by the continental shelf lithosphere, but high heat dissipation of mantle due to the Cretaceous breakup of Gondwana along the continent and ocean transition (COT), where large sediment ridges would be brought about by the Oligocene ice sheet retreat and would enlarge free-air gravity anomalies. In the western Ross Sea, CHINARE seismic profiles indicate northern termination of the Terror Rift and deposition time of the grounding zone wedge in the northern JOIDES Basin.

**Keywords** **marine geophysics, Chinese Polar Program, Antarctica, gravity, magnetics, seismic strata, Prydz Bay, Ross Sea**

**Citation**: Gao J Y, Shen Z Y, Yang C G, et al. Progress in Antarctic marine geophysical research by the Chinese Polar Program. Adv Polar Sci, 2017, 28 (4): 256-267, doi:10.13679/j.advps.2017.4.00256

## 1 Introduction

### 1.1 Brief history of Chinese Antarctic Marine Geophysical Expeditions

Chinese Antarctic marine geophysical expeditions occurred in two stages. During the first stage, from 1984 to 1991, there were only four cruises. During the second stage, starting with the Chinese Polar Environmental Comprehensive Investigation and Assessment Programs (known simply as the Chinese Polar Program) in 2011/2012, marine geophysical surveys have been undertaken every year.

* Corresponding author, E-mail: yangchunguo@sio.org.cn

### 1.1.1 The first stage from 1984 to 1991

The 1st Chinese National Antarctic Research Expedition (CHINARE) onboard the R/V *Xiangyanghong 10* in 1984/1985 collected bathymetric, gravimetric, and magnetic data in the Pacific Ocean, Drake Passage, Bransfield Strait, and Bellingshausen Sea. The 1st CHINARE deployed Chinese-made instruments ('683' bathymeter manufactured by Shanghai No.22 Radio Factory, DZY-2 marine gravimeter manufactured by Wuhan Institute of Seismology, State Earthquake Administration, and Jiujiang Instrument Factory, and CHHK-1 marine proton-procession magnetometer manufactured by Beijing Geological Instrument Factory) to obtain 3115 km of bathymetric, gravimetric, and magnetic lines in the Drake Passage, Bransfield Strait, and Bellingshausen Sea (Wu and Lv, 1988).

The 2nd CHINARE in 1985/1986, surveyed the Great Wall Bay by amphibious vehicle and inflatable rubber boat, completing the first 1:5000 bathymetric map of the bay (Song, 1987).

The 3rd CHINARE collected gravity data around the globe onboard the R/V *Jidi* in 1986/1987, marking the first shipborne expedition in the Atlantic and Indian Oceans by China (Wang et al., 1997).

Marine geophysical surveys were not performed during the 4th through 6th CHINARE between 1987/1988 and 1990/1991. The 7th CHINARE in 1991/1992 carried out a comprehensive geological and geophysical investigation in Bransfield Strait onboard the R/V *Haiyang 4*. The expedition acquired 43 geological samples, 5432 km of bathymetric lines, 4622.5 km of gravimetric lines, 2925.6 km of magnetic lines, and 2015 km of multi-channel seismic reflection lines on a 18 km by 36 km grid with line orientations of 333° and 53°, and also deployed two sonobuoys and collected data from them (Chen et al., 1995; Yao et al., 1995). The seismic source was a Chinese-made EH-4 air gun, but only 9 of the 48-channels in the streamer worked normally due to cold weather.

### 1.1.2 The second stage since 2011

Marine geophysical surveys were unfortunately interrupted during the 8th through 27th CHINARE for 20 years between 1991/1992 and 2011/2012. Since 2011, the R/V *Xuelong* icebreaker has spent 3—7 d annually for marine geophysical surveys around Antarctica (Chinese Arctic and Antarctic Administration, 2016).

In 2011/2012, the 28th CHINARE implemented a trial cruise for the Chinese Polar Program, acquiring 1375 km of bathymetric and gravity lines and 1111 km of magnetic lines at the eastern end of Bransfield Strait (Figure 1, Ma et al., 2015), and releasing and recovering 3 Chinese-made Ocean Bottom Seismometers (OBSs) in Prydz Bay.

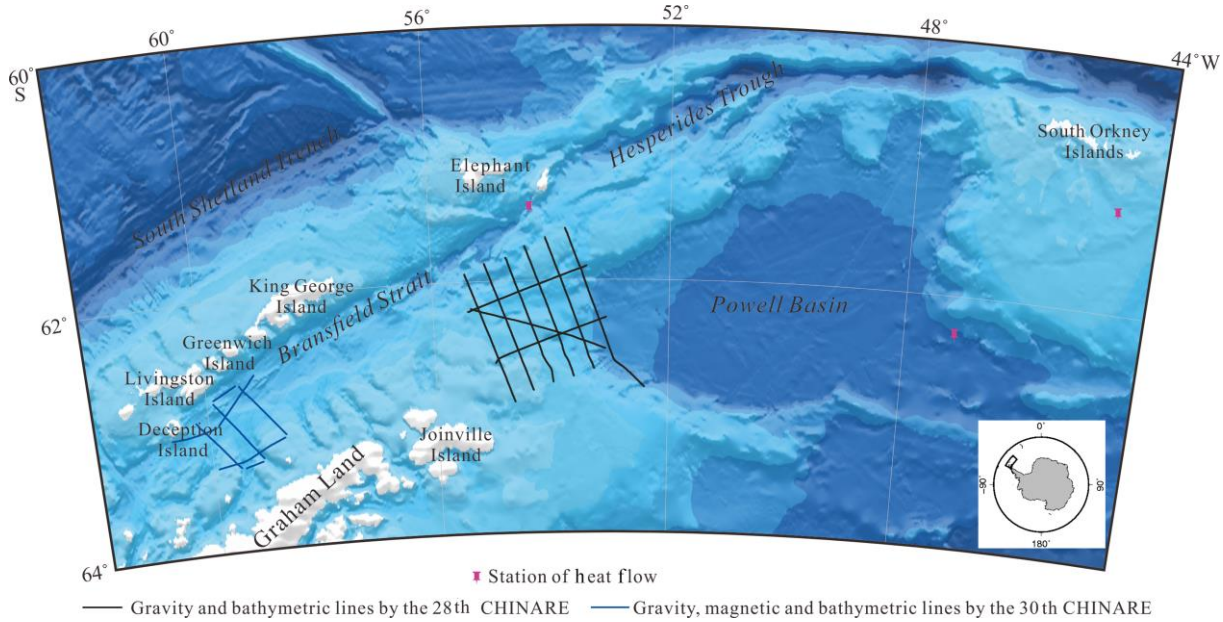


**Figure 1** Distribution of geophysical lines and stations implemented by the 28th and 30th CHINAREs in Bransfield Strait.

In 2012/2013, the 29th CHINARE implemented the first cruise offshore of Prydz Bay for the Chinese Polar Program, acquiring 2443 km of bathymetric and magnetic lines, and 2356 km of gravimetric lines (Figure 2). The expedition used a shipboard three-component magnetometer (STCM) together with 4 dual-frequency antennas of the Global Navigation Satellite System (GNSS) for shipborne magnetic measurement. In addition, 24-channel seismic reflection data were collected along three lines with a total length of 450 km. Five submarine heat flow stations and five Chinese-made long-period, wide-frequency OBSs were deployed along the 73°E line. This was the first Chinese integrated geophysical cruise ever to survey south of the Antarctic circle.

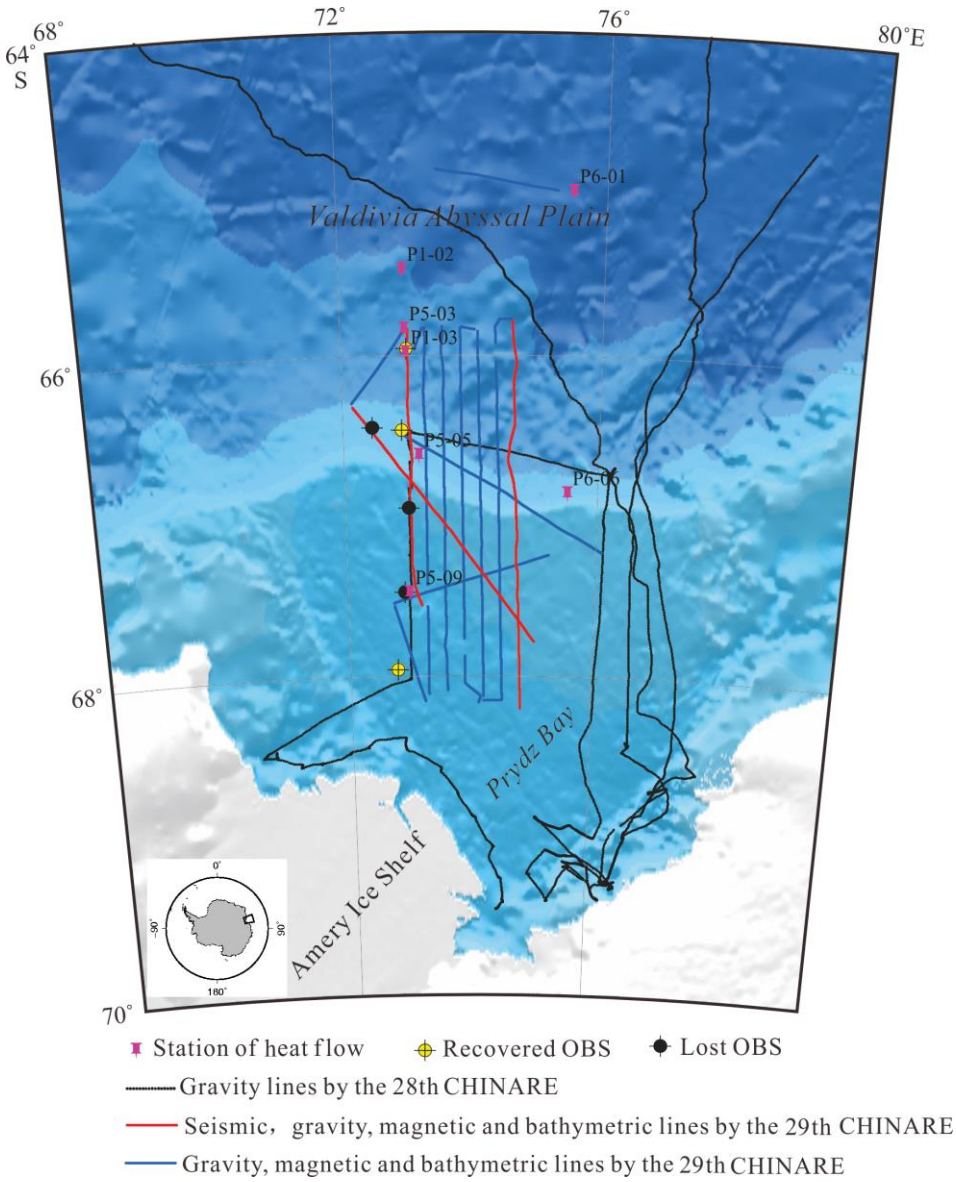


**Figure 2** Distribution of geophysical lines and stations implemented by the 28th and 29th CHINAREs offshore of Prydz Bay.

In 2013/2014, 2014/2015, and 2015/2016, the 30th, 31st, and 32nd CHINAREs implemented integrated geophysical surveys in the Ross Sea, undertaking high latitude research (Figure 3). During these three cruises, 1384.2 km of seismic profiles were obtained. The 30th and 31st CHINAREs acquired high-resolution 24-channel reflection seismic profiles using a Chinese-made streamer with a Chinese-made plasma spark source, and the 32nd CHINARE acquired medium-resolution 24-channel seismic reflection profiles with a 210 $in^3$ GI air-gun (with two chambers: a *g*eneral one and an injection one) connected to a Chinese-made 2000 psi air compressor. The 30th CHINARE collected 285.2 km of geophysical lines offshore of Terra Nova Bay (Figure 3) and 378.8 km of bathymetric, gravimetric and magnetic lines near Deception Island in Bransfield Strait (Figure 1), and deployed two heat flow stations offshore of Prydz Bay. The 31st CHINARE added 180 km of geophysical lines in the Drygalski Basin offshore of Terra Nova Bay and 229 km of nearly N-S trending geophysical line in the JOIDES Basin (Figure 3). The latter passed the Deep Sea Drilling Project (DSDP) site 273. The 31st CHINARE recovered three of the five OBSs released by the 29th CHINARE offshore of Prydz Bay, which had recorded more than 2500 global seismic events. Recovery of a Chinese-made OBS two years after release had never been attempted before this cruise. The 32nd CHINARE obtained 690 km of geophysical lines, connecting the 30th and 31st CHINARE lines in both the Drygalski and JOIDES basins to compare and date stratigraphy. During these three cruises, however, heat flow was not easily measured due to bottom water temperatures of less than −2°C in the Ross Sea.

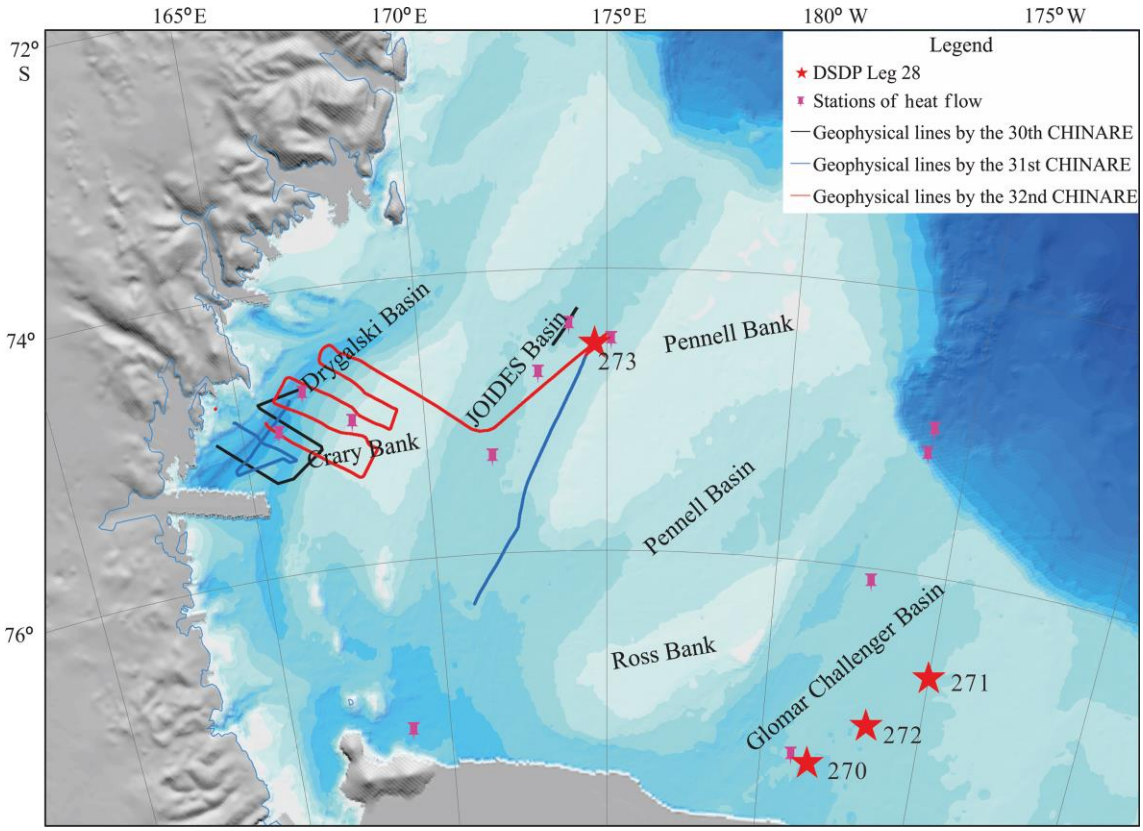


**Figure 3** Distribution of geophysical lines and stations implemented by the 30th, 31st, and 32nd CHINAREs in the Ross Sea.

# 2 Advances in Antarctic marine geophysical research by the Chinese Polar Program

## 2.1 Gravity anomalies and their implications for Antarctic geodynamics

To take advantage of gravity anomalies immediately relative to geodynamics, we have calculated and interpreted gravity anomalies for the whole Antarctic region, and particularly for offshore of Prydz Bay.

### 2.1.1 Calculation and interpretation of gravity anomalies for the whole Antarctica

Using surface elevation, ice thickness, and subglacial and submarine topography data from BEDMAP2 (Fretwell et al., 2013) and JGP95E (Arabelos, 1999), the global gravity terrain effects and Airy isostatic effects were calculated at each grid node in rectangular coordinates on an Antarctic polar azimuthal projection (Gao et al., 2015). Gravity terrain and isostatic effects from both near and far zones were repeatedly computed using the same formula for each truncated spherical shell. We also calculated Bouguer gravity anomalies (without gravity terrain effects) and Airy isostatic residual gravity anomalies (without gravity terrain and isostatic effects) for Antarctica and its surrounding seas (Figure 4) from the DTU10 global free-air gravity anomalies (Andersen, 2010). Free air anomalies are considerably influenced both by positive gravity effects from the Antarctic ice sheet and negative gravity effects from the Southern Ocean water. Bouguer anomalies (Figure 4a) reflect the influence of crustal isostatic compensation at the Moho surface, depressed under the continent and shoaling toward the margins (refer to Figure 5). Airy isostatic residual anomalies (Figure 4b) imply that the Antarctic continent and its surroundings are generally in isostatic equilibrium, although small scale bedrock relief is not locally compensated, especially in the Scotia Sea, East Antarctica, and the Indian Ocean.

For the Ross Sea sector and offshore of Wilkes Land, Airy isostatic residual anomaly change is generally smooth in the range of −40—0 mGal, with subtle positive values over the Transantarctic Mountains. Local Airy isostatic compensation seems reasonable, or even maybe over-compensated a little, in this region. Such isostatic behavior may be closely correlated with tectonic activities. The lithosphere under the Ross Sea and Wilkes Land near the Pacific-Antarctic Ridge is intensively broken by transform faults and the West Antarctic Rift System, and is not strong enough to support its own weight and favor local isostatic adjustment. To accurately and consistently compute Bouguer anomalies and Airy isostatic residual anomalies in the Antarctica and its surrounding seas, our grid data of global terrain and isostatic gravity effects can

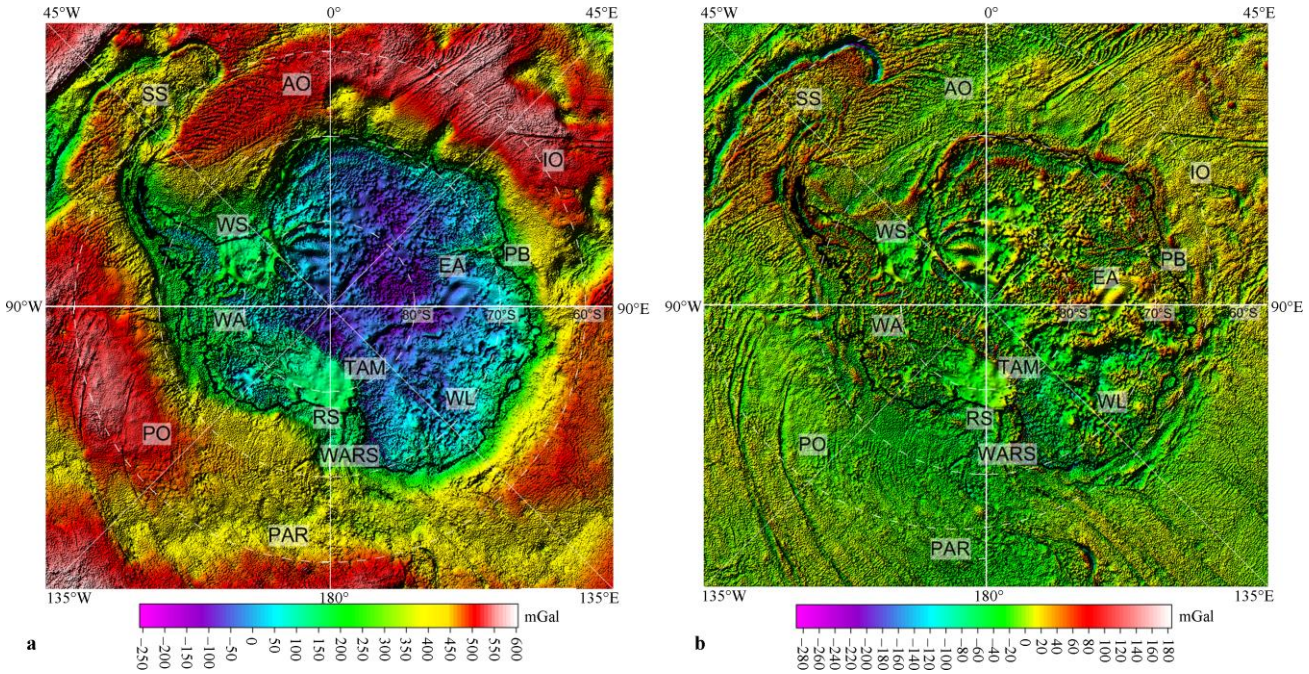


**Figure 4** Bouguer gravity anomalies (**a**) and Airy isostatic residual gravity anomalies (**b**) for Antarctica and its surrounding seas. AO = Atlantic Ocean; IO = Indian Ocean; PO = Pacific Ocean; EA = East Antarctica; WA = West Antarctica; PAR = Pacific-Antarctic Ridge; SS = Scotia Sea; WS = Weddle Sea; PB = Prydz Bay; RS= Ross Sea; WARS = West Antarctic Rift System; TAM = Transantarctic Mountains; WL = Wilkes Land.

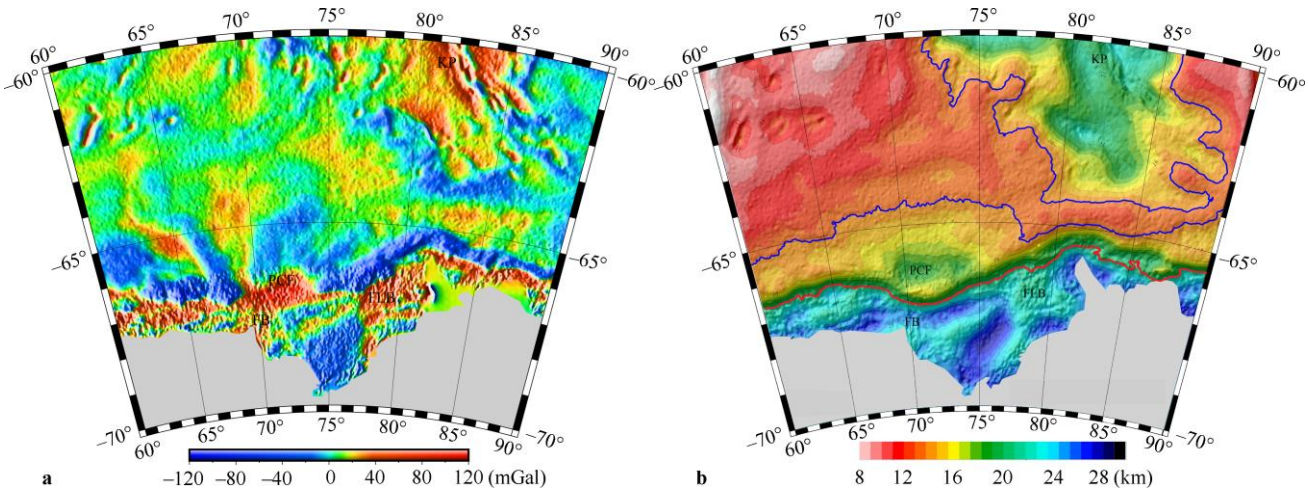


**Figure 5** Free-air gravity anomalies (**a**) and depths to the Moho (**b**) offshore of Prydz Bay. Red and blue contours represent depths of 22 km and 14 km to the Moho, respectively. KP = Kerguelen Plateau; PCF = Prydz Channel Fan; FLB = Four Ladies Bank; FB = Fram Bank.

be used to correct gravity anomalies from shipborne and airborne gravity surveys. Meanwhile, Bouguer anomalies and Airy isostatic residual anomalies computed from satellite altimetry gravity anomaly can be quantifiably inverted to interpret lithospheric density residuals, the Moho surface undulation and mantle dynamic information.

### 2.1.2 Inversion and interpretation of gravity anomalies for the Prydz Bay region

Free-air gravity anomalies merged from ship-borne gravity acquired by the 29th CHINARE and satellite altimetry gravity (Andersen, 2010) display the remarkable continental shelf edge effects offshore of Prydz Bay (Figure 5a), that is, a positive gravity zone along the continental slope or rise and a negative gravity zone on the oceanic basin side. The most distinctive feature is the large-scale gravity high over the Prydz Channel Fan (PCF) which overwhelms the negative gravity anomaly in this region. Basement depressions in the shelf basin are characterized by gravity lows. Four Ladies Bank and Fram Bank on the outer uplift zone of the continental shelf are indicated by disconnected gravity highs. These may imply

that deep lithospheric structures of the two banks were disrupted by the Lambert Rift before Antarctica separated from Gondwana.

After correcting for the gravitational effects of seawater (density of 1.03 $g \cdot cm^{-3}$), ice sheet (density of 0.9 $g \cdot cm^{-3}$), sedimentary cover (density compaction model of Sclater and Christie, 1990), and geothermal disturbance (Greenhalgh and Kusznir, 2007), the residual mantle Bouguer anomaly (RMBA) is calculated from the free-air gravity anomaly and used to infer depths to the Moho offshore of Prydz Bay (Figure 5b). On the Kerguelen Plateau, underlain with transitional oceanic crust (Ji et al., 2017), depths to the Moho fluctuate between 18 km and 23 km with crustal thicknesses exceeding 13 km. Within the oceanic basin, depths to the Moho range from 7 km to 14 km with crustal thicknesses between 5 km and 9 km. From the continent–ocean boundary (COB) to the continental shelf, depths to the Moho deepen from 14 km to 25 km. The contour depth of 22 km to the Moho depicts a sharply thinning belt of continental crust giving way to normal oceanic crust. The Moho is also uplifted in the Prydz Bay basin, which may be underlain with pre-Pan-African (800 Ma ago) sedimentary strata, metamorphosed to a certain degree in the upper crust. A series of faults cut through these sedimentary strata under the influence of the Prydz Bay orogeny. Accompanying the breakup of Gondwana, hypabyssal igneous rocks intruded into these faults as a result of decompression melting and increased the magnetic anomaly.

## 2.2 Magnetic, sedimentary and lithospheric features offshore of Prydz Bay

The 29th CHINARE cruise offshore of Prydz Bay collected more kinds and larger volumes of geophysical data than other cruises in the recent five years, as indicated in section 1.2. In combination with historical data, we have processed these data (Chinese Arctic and Antarctic Administration, 2016), and studied magmatic distribution, sedimentary strata and lithospheric anisotropy offshore of Prydz Bay.

### 2.2.1 Comparison of magnetic anomalies from shipborne and towed magnetometers

The 29th CHINARE performed O-shaped calibration loops for the interference field of the icebreaker R/V *Xuelong* and calculated the compensation coefficients for the STCM measurements offshore of Prydz Bay (Wang et al., 2017). The ship interference field computed from the compensation coefficients changes in the range of −3000—7000 nT with its different headings. By comparing the compensated magnetic anomaly from the STCM with those from the synchronously towed G880 magnetometer (manufactured by Geometrics Inc., San Jose, CA 95131, U.S.) and EMG2 grid data (NCEI Geomagnetic Modeling Team, 2015) (Figure 6), we found that the STCM has tolerable performance and reliability for tectonic studies on a polar continental shelf. Figure 6 shows that magnetic anomalies from three different sources have nearly identical undulations, ranging from −200 nT to 600 nT. In Figures 6a, 6b and 6c, there is a negative anomaly zone "i" less than −100 nT that extends east–northeast, a positive anomaly zone "ii" more than 300 nT which corresponds to the high magnetic anomaly zone of the Antarctic outer continental shelf, and a magnetic anomaly zone "iii" ranging from −100 nT in the west to 100 nT in the east with a near N–S strike. These three anomaly zones probably represent the magnetic quiet zone along the continental slope and rise, the mafic or ultramafic magmatism accompanied with the breakup of Gondwana and the seaward extension of the Lambert Rift away from Prydz Bay, respectively.

This is the first time Chinese scientists have collected STCM measurements in polar seas. Related technical refinements will provide effective support for the acquisition of the STCM data in upcoming Chinese polar expeditions.

### 2.2.2 Calculation and inference of continental margin anisotropy

When earthquake waves travel in an anisotropic medium, shear wave splitting into fast and slow waves with different polarization directions will occur. Using the rotation-correlation method (Bowman and Ando, 1987), Niu et al. (2016) have obtained shear wave splitting parameters offshore of Prydz Bay from five earthquakes recorded by three OBSs, deployed by the 29th CHINARE and recovered by the 31st CHINARE (Figure 7). At three OBS sites from north to south, the polarization directions of the fast shear wave are N40°E to N42°E, N44°E, and N52°E to N60°E, and the time delays between fast and slow shear waves are 0.8 s to 1.3 s, 0.2 s to 0.4 s, and 0.2 s to 0.8 s, respectively. The inversion results show strong anisotropy of the lithosphere at a scale of 50–150 km offshore of Prydz Bay with tensile strain striking SW–NE in the ocean and nearly E–W landward (Figure 7). The time delay between fast and slow shear waves is related to the anisotropic equivalent thickness of the lithosphere. The polarization direction and time delay would imply that oceanic anisotropy at OBS1 is dominated by mantle flow from mid-ocean ridge spreading, while continental anisotropy at OBS3 is dominated by the relict structural fabric of the ancient lithosphere at the top of the upper mantle. A shallow and thin anisotropy layer at OBS2 may imply weak activity of the COT mantle at present. The COT weak activity is consistent with low heat flow and low magnetic anomalies on the continental slope and rise, due to high heat dissipation of mantle during the breakup of Gondwana. Anisotropy deep within the upper mantle on the continental shelf is reflective of high heat flow and high magnetic anomalies west of Prydz Bay, due to high heat capacity of the mantle shielded by the Antarctic continental lithosphere.

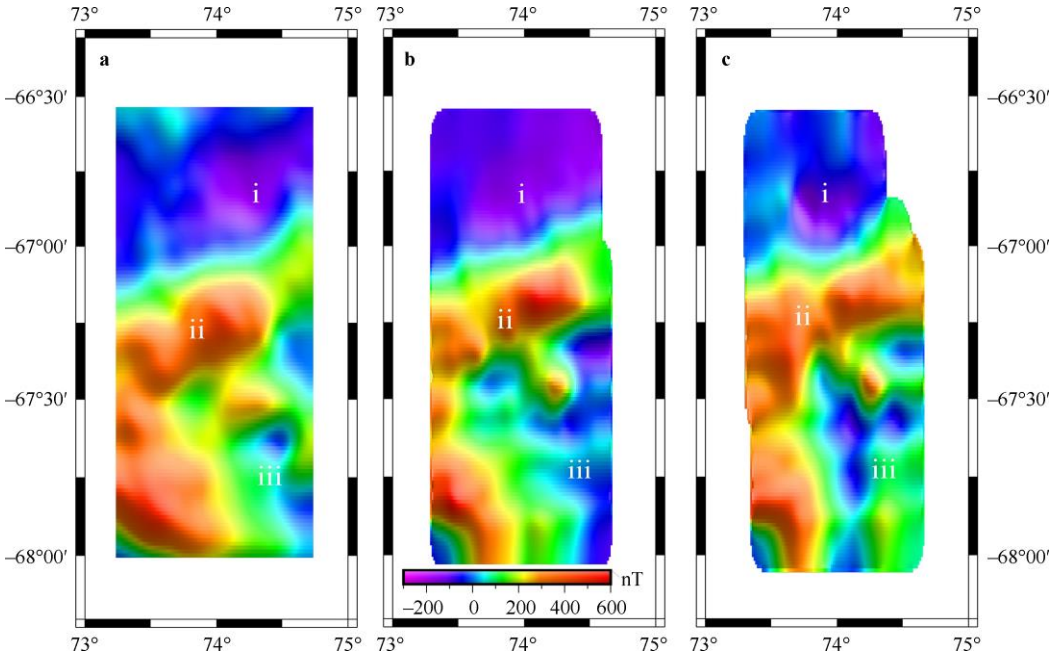


**Figure 6** Comparison of magnetic anomalies from three sources. **a**, EMAG2 from NGDC; **b**, Magnetic anomaly from the G880 towed magnetometer; **c**, Magnetic anomaly from the STCM.“i”representes the negative anomaly zone;“ii”representes the positive anomaly zone; “iii” representes the N–S trending anomaly zone.

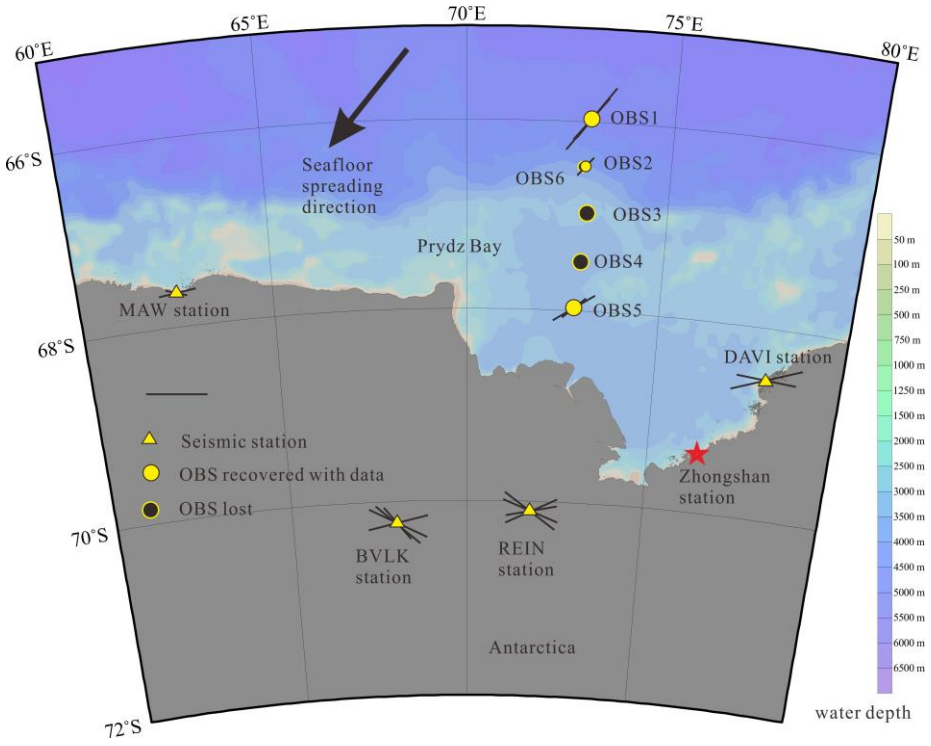


**Figure 7** Lithospheric anisotropy in the Prydz Bay region. MAW=Mawson, DAVI=Davis, BVLK=Beaver Lake, REIN= Reinbolt Hills (Refer to Reading and Heintz, 2008).

### 2.2.3 Development and influence of sediment ridges

The PCF (Figure 8a), located on the continental rise between 61°E and 75°E, consists of four sediment ridges (Daly SR, Wild SR, Wilkins SR and Murray-W SR) produced by turbidity currents. They are classified into two groups: Daly SR and Wild SR contain asymmetric levees on both sides of the Wild Canyon, Wilkins SR and Murray-W

SR contain eastward dipping denudation interfaces (local, diachronous hiatuses) in the Wilkins and Murray canyons. The bottom of the 1165C hole from the ODP 118 cruise (Cooper and O'Brien, 2004) is 999 m deep and dated at 21.2±0.1 Ma (Williams and Handwerger, 2005). Given a 93.6 m·Ma$^{-1}$ sedimentation rate through the hole bottom (Florindo et al., 2003) to the depth of the P3 event and 2840 m·s$^{-1}$ seismic velocity (Shipboard Scientific Party, 2001), the P3 event would have occurred at 26.1 Ma (Shen et al., 2015), corresponding to the end of the cooling and glacial epoch that began at the Eocene-Oligocene transition. The PCF sediment ridges were deposited after the P3 event (Figure 8b), when the Antarctic ice sheet retreated and meltwater-till flows and turbidity currents scoured the continental shelf and slope. Original ice-eroded troughs or canyons became main channels for turbidity currents, boosting development of the sediment ridges. Meanwhile, enormous amounts of meltwater would converge into a cold, dense water mass spilling down to the slope foot and further enhance sediment waves after the P3 event. It can be concluded that massive deposition in the PCF sediment ridges is linked to global climate warming and retreat of the Antarctic ice sheet during the late Oligocene and early Miocene.

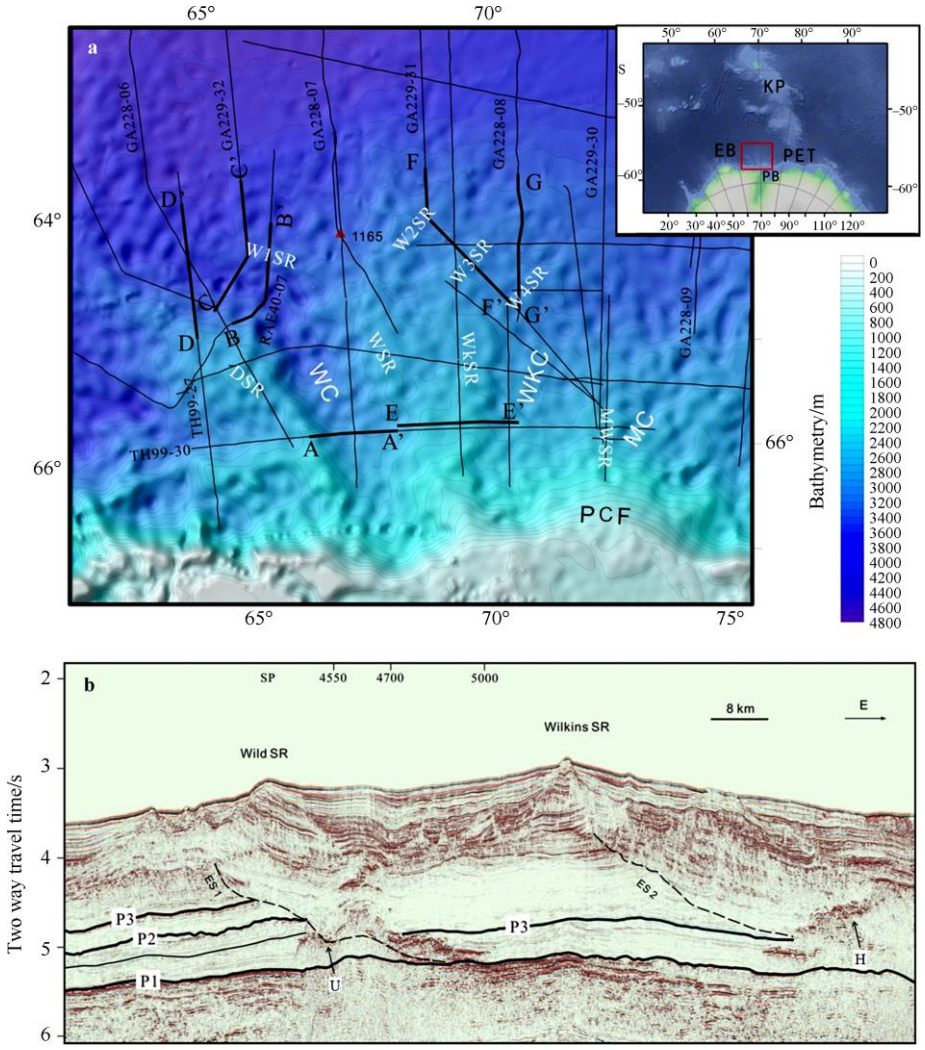


**Figure 8** Topography (**a**) and sediment structure along line EE′ (**b**) of the Prydz Channel Fan. Seismic profiles are from the Antarctic Seismic Data Library System (SDLS, Wardell, 2017). U: U reflection; H: high-amplitude reflection that migrates eastward; ES1, ES2: erosion surface. SR = sediment ridge, DSR = Daly SR, WSR = Wild SR, WKSR = Wilkins SR, MWSR = Murray-W SR; WC = Murray Channel, WKC = Wilkins Channel, MC = Murray Channel; PET = Princess Elizabeth Land Trough; EB =Enderby Basin; KP = Kerguelen Plateau; PB = Prydz Bay.

Effective elastic thickness ($T_e$) of the lithosphere was about 20 km in the PCF region (Dong et al., 2013) where the sediment ridges were deposited during the P3 event. PCF occurred much later than rifting of the Prydz Bay continental margin during the Cretaceous, with low $T_e$. The PCF free-air gravity anomaly high (Figure 5a) may have originated from the sediment ridges, because the cooled lithosphere beneath the PCF had high $T_e$ (or mechanical

strength) to support massive deposition after the late Oligocene; that is, crust could not be flexed enough to compensate for the weight of the PCF sediment ridges.

### 2.3 Rift structure and glaciomarine sedimentation in the western Ross Sea

Sparker seismic profiles acquired by the 30th and 31st CHINAREs and GI-airgun seismic profiles acquired by the 32nd CHINARE are mainly located in the northern JOIDES and northern Victoria Land Basins. These seismic profiles, combined with core sample from the 31st CHINARE and related research (Halberstadt et al., 2016; Hall et al., 2007; Henrys et al., 2007; Domack et al., 1999), highlight the northern termination of the Terror Rift and the front of glacial grounding line in the JOIDES Basin.

#### 2.3.1 Tracing and defining structures in the northern Terror Rift

Based on densely arranged seismic profiles, Hall et al. (2007) and Henrys et al. (2007) mapped structural elements in the southern and central part of Terror Rift in detail (Figure 9a). In contrast to Cooper's (1987) point of view, they found that the Lee Arch, near the Drygalski ice tongue, is a nearly N–S striking roll anticline and not related to magma intrusion. There is no evidence of strike-slip fractures shown on new seismic profiles of higher quality (Hall et al., 2007). Some previously defined strike-slip faults (Salvini et al., 1997), partly attributed to poor quality or low resolution of seismic profiles, can be also interpreted as grabens. On our ant32-01 seismic profile north of the Drygalski ice tongue (Figure 9c), Terror Rift shows no sign of magma intrusion, but exhibits rolling and falling half-grabens tilted by normal faults on the eastern slope. On our ant32-05 seismic profile far to the north of the Drygalski ice tongue (Figure 9b), normal faults disappear, and the northernmost end faulting associated with Terror Rift may not pass by north of 74°30′S.

#### 2.3.2 Depicting and dating a grounding-zone wedge in the northern JOIDES Basin

In the northern JOIDES Basin (between 75.0°S and 74.2°S), Halberstadt et al. (2016) found a huge grounding-zone wedge sedimentary body (GZW J1), that is a combination of a grounding line of an ice sheet or cap formed during the last glacial maximum (LGM) and a sedimentary wedge deposited during the following deglaciation (Figure 10b). We name the front of GZW J1 as GZW J1-1, through which our ant30-01 seismic profile (Figure 10a) passes. GZW J1-1 is mainly composed of seismic sequence U2, a transparent layer between SN (shot number) 600 and SN 1750 along the profile, covered by seismic sequence U1, a thin blanket of parallel reflection with SWT (single way travel) of about 4 ms. Along the profile (Figure 10a), Z1 marks the location of core JB06 sampled by the 31st CHINARE (Huang et al., 2016), and Z2 marks the location of two cores NBP9401 017-pc and NBP9501 039-kc (Domack et al., 1999). The bottom age of core JB06, 2.99 m in length, is extrapolated to be 33.6 ka (Huang et al., 2016); while sediments dated 30.2 ka are found at the depth of 10 cm to 12 cm for NBP9401 017-pc, which was 3.66 m in length (Domack et al., 1999). Assuming a seawater seismic velocity of 1500 $m \cdot s^{-1}$, the uppermost seismic sequence U1 of the sedimentary grounding zone wedge is 6 m thick, twice the depths of the 30.2 ka to 33.6 ka ages from these cores (Huang et al., 2016; Domack et al.,1999). It can be deduced that the main body U2 of GZW J1-1 had been deposited long before 30.0 ka, instead of during or after the LGM (26.0 ka to 19.0 ka). Hence, the Antarctic ice sheet during the LGM did not reach the front of GZW J1 as captured by our ant30-01 seismic profile in the northern JOIDES Basin.

## 3 Summary

We can make a brief summary on Chinese Antarctic marine geophysical research on basis of analysis described above:

(1) After a 20 year hiatus, Chinese scientific activities in marine geophysics have returned to Antarctic waters annually since 2011/2012. During the last 5 years, we have acquired a total of 5581 km of bathymetric lines, 5494 km of gravimetric lines, 5389 km of magnetic lines, and 1834 km of 24-channel seismic reflection lines around Antarctica, including data from eight heat flow stations and three OBS stations. In the western Ross Sea, a total of 1380 km of mid and high resolution seismic profiles have been acquired. Leveraging this data acquisition, we have obtained five grants from the National Natural Science Foundation, published one book, and authored a series of Antarctic marine geophysical research manuscripts.

(2) Compiled Antarctic Bouguer and Airy isostatic residual gravity anomalies provide insight into the striking differences of tectonics between the East Antarctic stability and West Antarctic activity. As a stable craton with better regional isostatic compensation, East Antarctica is characterized by large scale, lower Bouguer anomalies. Meanwhile, small scale, higher isostatic residual anomalies of East Antarctica imply its poorer local isostatic compensation. Large scale mean Bouguer anomalies and lower isostatic residual anomalies for the Ross Sea sector and offshore of Wilkes Land may reflect neo-tectonic activities and mantle magmatism related to the Pacific–Antarctic Ridge and the West Antarctic Rift System.

(3) Magnetic anomalies acquired from the STCM and towed magnetometer consistently display an elevated magnetic anomaly zone along the Prydz Bay outer shelf. This zone implies volcanism during the breakup of Gondwana, also verified by high isostatic residual gravity anomalies. High western, and low eastern, magnetic anomalies

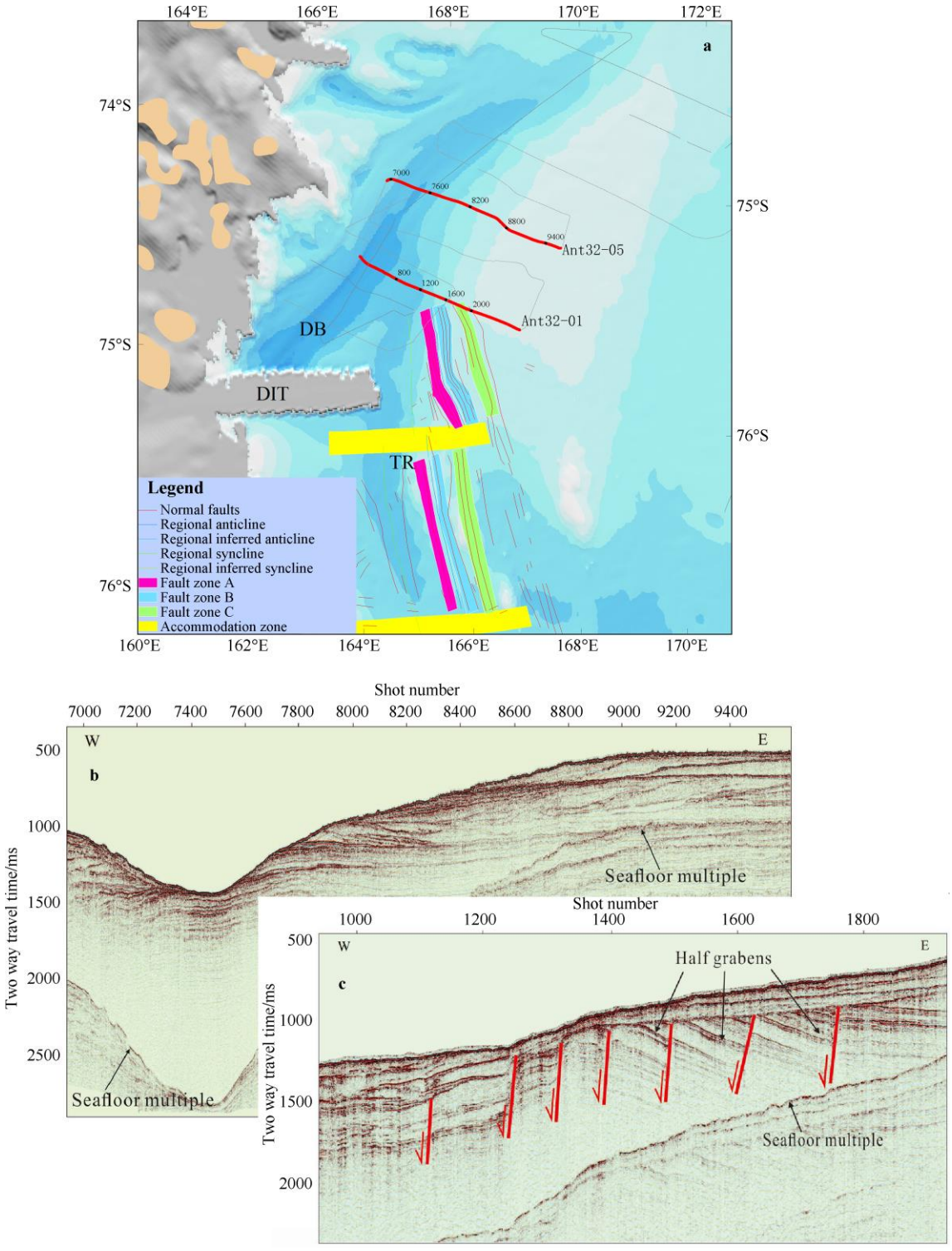


**Figure 9** Northern termination of the Terror Rift (**a**) expressed by ant32-05 (**b**) and ant32-01 (**c**) seismic profiles. TR = Terror Rift; DIT = Drygalsky ice tongue; DB = Drygalsky Basin. Tectonic structures of the central Terror Rift refer to Hall et al. (2007).

on the Prydz Bay inner shelf may imply seaward extension of the Lambert Rift earlier than the breakup of Gondwana. The continental shelf shear wave anisotropy deep in the upper mantle is consistent with high heat flow and high magnetic anomalies west of Prydz Bay, due to high heat capacity of the mantle shielded by continental lithosphere. The shallow anisotropy on the Prydz Bay continental slope and rise is consistent with low heat flow and low magnetic anomalies, due to high heat dissipation of the mantle during the Cretaceous breakup of Gondwana. The PCF

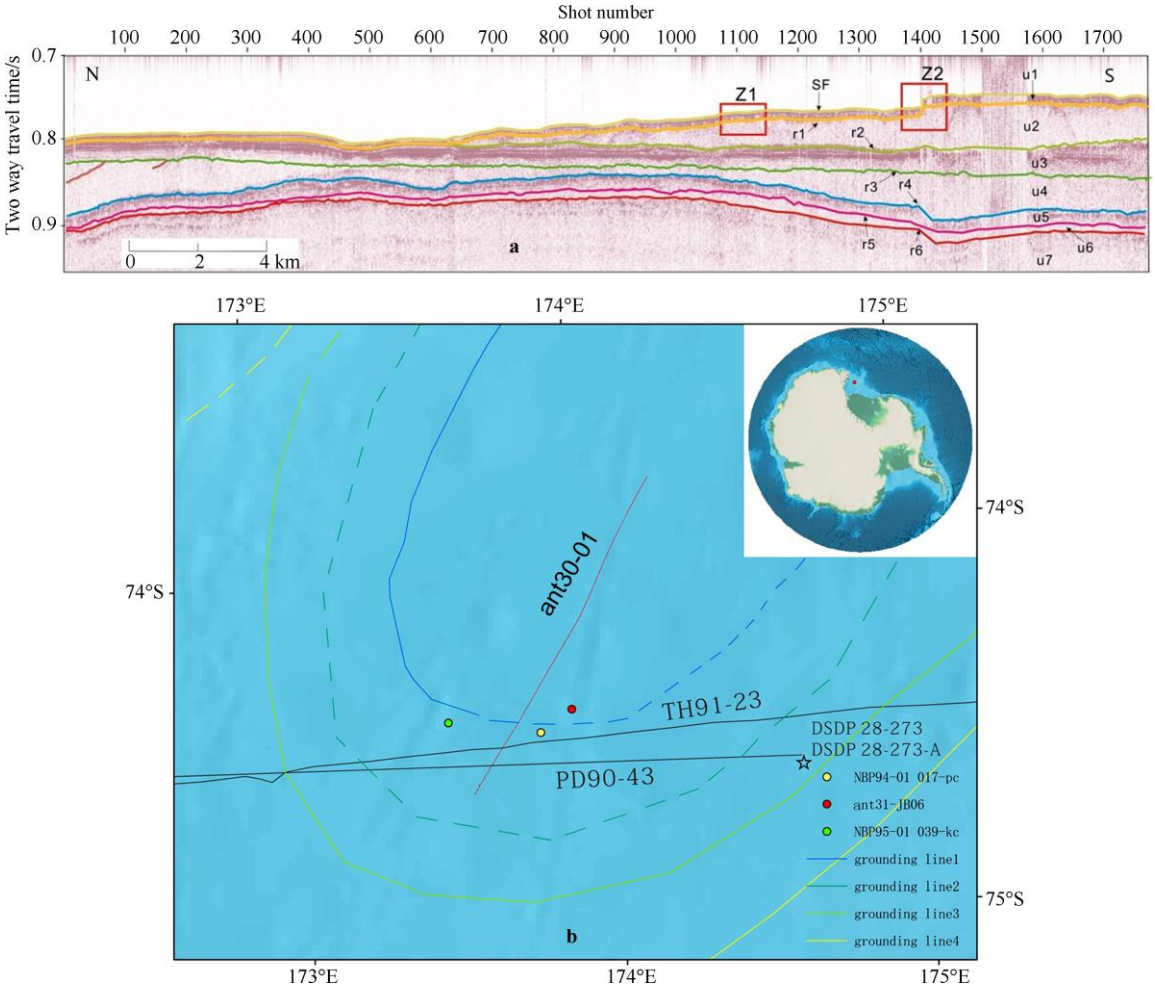


**Figure 10** The grounding-zone wedge captured by ant30-01 seismic profile (**a**) in the northern JOIDES Basin (**b**). SF is the sea bottom; r1, r2, r3, r4, r5, r6 are seismic reflections dividing seismic sequences u1, u2, u3, u4, u5, u6, u7. Z1, Z2 are locations of cores ant31-JB06, NBP94-01 017-pc and NBP95-01 039-kc mapping on the ant30-01 seismic line. The grounding line1, line2, line3 and line4 refer to Halberstadt et al. (2016).

sediment ridges deposited on cold and hard lithosphere with high $T_e$ when the Oligocene ice sheet retreated, creating the PCF free-air gravity anomaly high.

(4) In the western Ross Sea, CHINARE seismic profiles indicate rolling and falling half-grabens tilted by normal faults on the eastern slope of the northern Terror Rift, the northern end of which may not extend north of 74°30′ S. CHINARE seismic profile captures the front of a sedimentary grounding zone wedge deposited before the last glacial maximum in the northern JOIDES Basin.

**Acknowledgments** This study is financially supported by the National Natural Science Foundation of China (Grant Nos. 41576069, 41306201, 41776189, 41706212 and 41706215), the Chinese Polar Environment Comprehensive Investigation & Assessment Programs (Grant Nos. CHINARE2017-01-03 and CHINARE2017-04-01), and the Special Foundation of the Second Institute of Oceanography, SOA (Grant No. 14260-10). We thank two anonymous reviewers and an editor, for reviewing this manuscript.

## References

Andersen O B. 2010. The DTU10 Gravity field and Mean sea surface. Second international symposium of the gravity field of the Earth (IGFS2). Fairbanks, Alaska: University of Alaska Fairbanks

Arabelos D. 1999. Intercomparisons of the global DTMs ETOPO5, Terrain Base and JGP95E. the XXIV general assembly of the EGS, the Hague, 19–23 April, 1999

Bowman J R, Ando M. 1987. Shear-wave splitting in the upper-mantle wedge above the Tonga subduction zone. Geophys J Int, 88(1): 25–41, doi: 10.1111/j.1365-246X.1987.tb01367.x

Chen S Y, Liu F L, Liang D H. 1995. Geophysical field and geologic structure of the Bransfield Sea area in the Antarctic circle. Mar Geol Quat Geol, 17(1): 77–86 (in Chinese)

Chinese Arctic and Antarctic Administration (CAA). 2016. Report of

marine geophysical expedition in the Antarctic surrounding seas. Beijing: China Ocean Press (in Chinese)

Cooper A K, Davey F J, Behrendt J C. 1987. Seismic stratigraphy and structure of the victoria Land Basin, Western Ross Sea, Antarctica//Cooper A K, Davey F J. The Antarctic continetal margin: geology and geophysics of the Western Ross Sea, CPCEMR Earth Series, Volume 5B. Houston, Texas: Circum-Pacific Council for Energy and Mineral Resources

Cooper A K, O'Brien P E. 2004. Leg 188 synthesis: transitions in the glacial history of the Prydz Bay region, East Antarctica, from ODP drilling//Cooper A K. O'Brien P E, Richter C. Proceedings of the Ocean Drilling Program, Scientific Results, Volume 188. College Station, TX, 1–42

Domack E W, Jacobson E A, Shipp S, et al. 1999. Late Pleistocene–Holocene retreat of the West Antarctic Ice-sheet system in the Ross Sea: part 2—sedimentologic and stratigraphic signature. Geol Soc Am Bull, 111(10): 1517–1536

Dong C Z, Ding W W, Li J B, et al. 2013. The Gravity and magnetic anomaly and crustal structure of Prydz Bay, East Antarctica. Chinese J Geophys, 56(10): 3346–3360 (in Chinese)

Florindo F, Bohaty S M, Erwin P S, et al. 2003. Magnetobiostratigraphic chronology and palaeoenvironmental history of Cenozoic sequences from ODP sites 1165 and 1166, Prydz Bay, Antarctica. Palaeogeogr, Palaeoclimatol, Palaeoecol, 198(1–2): 69–100

Fretwell P, Pritchard H D, Vaughan D G, et al. 2013. Bedmap2: improved ice bed, surface and thickness datasets for Antarctica. Cryosphere, 7(1): 375–393

Gao J Y, Yang C G, Zhang T, et al. 2015. Calculation of terrain and isostatic gravity effects in Antarctica and its surroundings. Hydrogr Surv Chart, 35(3): 1–7, doi: 10.3969/j.issn.1671-3044.2015.03.001 (in Chinese)

Greenhalgh E E, Kusznir N J. 2007. Evidence for thin oceanic crust on the extinct Aegir Ridge, Norwegian Basin, NE Atlantic derived from satellite gravity inversion. Geophy Res Lett, 34(6): L06305, doi: 10.1029/2007GL029440

Halberstadt A R W, Simkins L M, Greenwood S L, et al. 2016. Past ice-sheet behaviour: retreat scenarios and changing controls in the Ross Sea, Antarctica. Cryosphere, 10(3): 1003–1020

Hall J M, Wilson T W, Henrys S. 2007. Structure of the central Terror Rift, western Ross Sea, Antarctica//Cooper A K, Raymond C R. Antarctica: a keystone in a changing world–online proceedings of the 10th ISAES. USGS OFR-2007–1047, Short Research Paper 108. U.S. Geological Survey, doi: 10.3133/of2007-1047.srp108

Henrys S A, Wilson T J, Whittaker J M, et al. 2007. Tectonic history of mid-Miocene to present southern Victoria Land Basin, inferred from seismic stratigraphy in McMurdo Sound, Antarctica//Cooper A K, Raymond C R. Antarctica: a keystone in a changing world—online proceedings for the 10th ISAES. USGS OFR-2007–10477, Short Research Paper 049. U.S. Geological Survey, doi: 10.3133/of2007-1047.srp049

Huang M X, Wang R J, Xiao W S, et al. 2016. Retreat process of Ross Ice Shelf and hydrodynamic changes on northwestern Ross continental shelf since the last glacial. Mar Geol Quat Geol, 36(5): 97–108 (in Chinese)

Ji F, Gao J Y, Zhang T, et al. 2017. Spatial variations of lithospheric effective elastic thickness over Kerguelen plateau. Prog Geophys, 32(1): 48–55, doi: 10.6038/pg20170106 (in Chinese)

Ma L, Zheng Y P, Pei Y L, et al. 2015. The adjustment of shipborne gravimetric data for the Bransfield Strait. Adv Mar Sci, 33(3): 403–413 (in Chinese)

NCEI Geomagnetic Modeling Team. 2015. (2015-08-31) [2017-08-31]. EMAG2: earth magnetic anomaly grid (2-arc-minute resolution). https://www.ngdc.noaa.gov/docucomp/page?xml=NOAA/NESDIS/NGDC/MGG/Geophysical_Models/iso/xml/EMAG2.xml&view=getDataView&header=none

Niu X W, Gao J Y, Wu Z C, et al. 2016. Lithosphere anisotropy of Prydz Bay, Antarctica: from ocean bottom seismometer long term observation. Earth Sci, 41(11): 1950–1958, doi: 10.3799/dqkx.2016.135 (in Chinese)

Reading A M, Heintz M. 2008. Seismic anisotropy of East Antarctica from shear–wave splitting: spatially varying contributions from lithospheric structural fabric and mantle flow? Earth Plant Sci Lett, 268 (3–4): 433–443

Salvini F, Brancolini G, Busetti M, et al. 1997. Cenozoic geodynamics of the Ross Sea region, Antarctica: crustal extension, intraplate strike-slip faulting, and tectonic inheritance. J Geophys Res, 102(B11): 24669–24696

Sclater J G, Christie P A F. 1980. Continental stretching: an explanation of the post-mid-cretaceous subsidence of the central North Sea basin. J Geophys Res, 85(B7): 3711–3739

Shen Z Y, Yang C G, Gao J Y, et al. 2015. Structure and development processes of the sediment ridges on the continental rise off the Prydz Bay margin, East Antarctica. Acta Geoscient Sin, 36(6): 709–717 (in Chinese)

Shipboard Scientific Party. 2001. Leg 188 summary: Prydz Bay—Cooperation Sea, Antarctica//O'Brien P E, Cooper A K, Richter C, et al. Proceedings of the ocean drilling program, initial reports, volume 188. College Station, TX: Ocean Drilling Program, 1–65

Song D K. 1987. Geomorphology of the beach and sea floor relief features of the Great Wall Bay in Antarctica. Mar Sci, 11(4): 18–21 (in Chinese)

Wang S G, Liu Z C, Wu J L. 1997. Gravity anomalies and their tectonic implications of mid-ocean ridges in the Pacific, Atlantic and Indian Oceans. Acta Oceanol Sin, 19(6): 94–101 (in Chinese)

Wang W J, Gao J Y, Wu Z C, et al. 2017. Processing and analyses on shipboard three-component magnetometer data from Prydz Bay, Antarctica. Chin J Polar Res, 29 (3): 349-346, doi: 10. 13679/j.jdyj.2017.1.349

Wardell N G. 2017. Antarctic seismic data library system.[2017-8-28]. http://www.ogs.trieste.it/en/content/antarctic-seismic-data-library-system

Williams T, Handwerger D. 2005. A high-resolution record of early Miocene Antarctic glacial history from ODP Site 1165, Prydz Bay. Paleoceanography, 20(2): PA2017, doi: 10.1029/2004PA001067

Wu S G, Lv W Z. 1988. The history of spreading of darke passage and its effects. Antarct Res, 1(2): 1–7 (in Chinese)

Yao B C, Wang G Y, Chen B Y, et al. 1995. The characteristics of geophysical field and tectonic evolution in the Bransfield Strait. Antarct Res (Chin Ed), 7(1): 25–35 (in Chinese)